Stem Cell Research & Therapy

RESEARCH

Open Access

Xenogenous implanted dental follicle stem cells promote periodontal regeneration through inducing the N2 phenotype of neutrophils

Li Liu[1,2,3,4,5*], Yuqi Wen[1,2,3,4,5], Liangrui Chen[1,2,3,4,6], Maoxue Li[1,2,3,4,5], Jialu Yu[1,2,3,4,6], Weidong Tian[1,2,3,4,6], Yafei Wu[1,2,3,4,5*] and Shujuan Guo[1,2,3,4,5*]

Abstract

Background Periodontal tissue loss is the main reason for tooth mobility and loss caused by periodontal disease. Dental follicle stem cells (DFSCs) have significant therapeutic potential in periodontal regeneration, which maybe mainly depends on their potent immunomodulatory capacity. Consequently, this study aims to elucidate the impact of implanted xenogenous DFSCs on innate immune responses during early and late stages in the periodontal defect repair period.

Methods To trace and investigate the immunomodulation mechanisms of DFSCs in vivo, DFSCs were engineered (E-DFSCs) using lentiviral vectors expressing CD63-enhanced green fluorescent protein (CD63-EGFP) and β-Actin-mCherry protein (ACTB-mCherry) to exhibit green and red fluorescence. The biological characteristics and functions of E-DFSCs were verified by proliferation, differentiation, and co-culture experiments in vitro. In vivo, the periodontal regeneration capacity of E-DFSCs was detected by implantation of murine periodontal defect model, and the response of innate immune cells was detected at the 1st, 3rd, and 5th days (early stage) and 4th week (late stage) after implantation.

Results In vitro assessments showed that E-DFSCs retain similar properties to their non-engineered counterparts but exhibit enhanced macrophage immunomodulation capability. In mice models, four-week micro-CT and histological evaluations indicated that E-DFSCs have equivalent efficiency to DFSCs in periodontal defect regeneration. At the early stage of repair in mice periodontal defect, fluorescence tracking showed that implanted E-DFSCs might primarily activate endogenous cells through direct contact and indirect actions, and most of these cells are myeloperoxidase-positive neutrophils. Additionally, compared with the control group, the neutrophilic infiltration and conversion of N2-type were significantly increased in the E-DFSC group. At the late stage of defect regeneration, more M2-type

*Correspondence:
Li Liu
liuli2@stu.scu.edu.cn
Yafei Wu
yfw1110@163.com
Shujuan Guo
guoshujuan@scu.edu.cn

Full list of author information is available at the end of the article

macrophages, fewer TRAP + osteoclasts, and an upregulated OPG/RANKL ratio were detected in the E-DFSC group compared to the control group, which indicated that immune balance tilts towards healing and bone formation.

Conclusion The xenogenous implanted DFSCs can induce the N2 phenotype of neutrophils in the early stage, which can activate the innate immune mechanism of the host to promote periodontal tissue regeneration.

Keywords Dental follicle stem cells, Periodontal regeneration, Cell tracing, Cell transplantation, Neutrophil, Macrophage, Immune regulation

Introduction

Periodontitis, a highly prevalent oral infectious disease, is characterized by the formation of periodontal pockets, attachment loss, and alveolar bone resorption, ultimately leading to tooth loss [1]. Additionally, periodontal infection is linked to systemic diseases such as cardiovascular diseases, diabetes [2], and Alzheimer's disease [3], posing significant risks to overall health. Although current clinical treatments effectively manage pathogenic bacteria and inflammation, they are insufficient for the repair of defects in soft and hard periodontal tissues caused by periodontitis [4]. The presence of periodontal defects will repeatedly induce periodontitis activity and promote disease progression. Traditional surgical interventions employ primitive stem cells to create new periodontal attachments; however, the local inflammatory microenvironment often impairs the functionality of these cells, hindering periodontal regeneration [5, 6]. Recently, cell therapy has emerged as a prominent direction in periodontal tissue engineering research, with the local transplantation of exogenous stem cells showing efficacy in enhancing periodontal regeneration [6].

Dental follicle stem cells (DFSCs), recognized as ideal seed cells, are harvested from tissues in the tooth germ developmental stage and exhibit capabilities such as self-renewal, multi-differentiation, migration, colonization, and immunoregulation [7]. They also offer advantages for periodontal regeneration due to their abundant sources, ease of expansion, and low immunogenicity [8]. The efficacy of DFSCs in promoting periodontal regeneration in animal models of periodontitis or periodontal defects has been confirmed, although the specific mechanisms remain to be elucidated [7, 9–11]. Numerous studies have explored the functional mechanisms of mesenchymal stem cells (MSCs) post-implantation in vivo, proposing various theories [12]. As research advances, the initial trans-differentiation mechanism struggles to account for the brief survival of implanted xenogeneic and allogeneic MSCs, as well as the disparity between the sites of periodontal regeneration and cell implantation [13]. Recent investigations increasingly suggest that MSCs likely facilitate tissue regeneration by directly interacting with primitive cells [14, 15] and indirect paracrine effects of secreting bioactive substances [13]. These phenomena modulate both innate and adaptive immune responses and prompt native tissue cells to repair damaged tissues, [13–17] thereby enabling the orderly progression of inflammatory necrotic tissue clearance and neo-tissue regeneration.

However, the majority of research on the mechanisms by which MSCs promote periodontal regeneration in vivo tends to be results-oriented. Typically, after MSCs implantation, selected indicators are measured in samples at specific time points, often aligned with the healing cycles of animal models [10, 11]. For instance, Lu [18] et al. reported that local injections of bone marrow stem cells (BMSCs) could suppress osteoclast activity and the RANKL/OPG ratio, thereby enhancing periodontal regeneration, as determined by histological analysis of mouse periodontium four weeks post-implantation. The survival of implanted MSCs in vivo is brief, with approximately 40% of cells persisting by the seventh day in the cells sheet [9]. Consequently, using regeneration outcomes to determine observational time points may not effectively elucidate the initial mechanisms of MSCs' action, given that many MSCs do not survive to the completion of periodontal regeneration. While some studies, such as those by Wei [9] and Liu [16], have opted for earlier time points, their focus has been limited to macrophages, which are less prevalent, rather than a broader spectrum of immune cells. For example, recently, more and more damage model studies have found that neutrophils in innate immunity play a significant role in the process of tissue regeneration and repair [19–22]. Similarly, some studies have shown that a series of biological behaviors of neutrophils in the process of immune response can directly or indirectly promote periodontal tissue regeneration, such as involving M2-type macrophage polarization to alleviate bone loss [16, 19], forming NETs to act as a scaffold for bone regeneration [21] and secreting SDF-1 [23] and VEGF [24] to drive stem cell migration and vascular regeneration. Additionally, studies confirmed that PDLCs can regulate neutrophil immune clearance through the paracrine effect during co-culture [25, 26], and Xu [27] et al. found that PDLCs strengthened by PCL/LAP nanofiber membrane could promote the N2 transformation of neutrophils in vitro and showed stronger periodontal regeneration ability in vivo. This raises questions about whether the detected

target cells are the primary mediators that interact with implanted MSCs and contribute to tissue repair.

To further investigate the following aspects in vivo, including the fate of implanted DFSCs, the mechanism of stimulating endogenous cells in periodontal tissue, and the effect on the regulation of periodontal innate immunity, this study employs a novel approach. DFSCs will be marked using dual-fluorescent CD63-EGFP and ACTB-mCherry labels to track the fate and interaction with endogenous cells of implanted DFSCs. This research aims to provide experimental evidence and a foundational understanding of the potential mechanisms by which DFSCs contribute to periodontal regeneration.

Materials and methods

All cell cultures and animal experiments conducted in this study were reviewed and approved by the Ethics Committees of the West China School of Stomatology, Sichuan University (No. WCHSIRB-D-2023-422 for human dental follicle tissue acquisition and No. WCHSIRB-D-2023-038 for animal experiments). Written informed consents were obtained from patients and their families who provided teeth for further research. All experimental animals were sourced from Chengdu Dassy Experimental Animals Co., Ltd., China.

Cell culture

Dental follicle tissues were harvested from the immature mandibular third molars, and periodontal ligament tissues were collected from premolars removed from teenagers aged 12–25 undergoing orthodontic treatment. Detailed protocols for the isolation and culture of DFSCs and periodontal ligament cells (PDLCs) follow those described in previous studies [28, 29]. Cells from passages 2 (P2) to 5 (P5) will be utilized in subsequent experiments. Mouse macrophage RAW264.7 cells were acquired from the Type Culture Collection Committee of the Chinese Academy of Sciences (ATCC), and culture conditions are detailed in a previous publication [29].

Lentivirus infection

Following preliminary experimentation, the minimum multiplicity of infection (MOI) required to achieve over 80% infection of DFSCs was determined to be 30 for the CD63-enhanced green fluorescent protein-puromycin resistance (CD63-EGFP-Puro) lentivirus and 15 for the β-Actin-mCherry-Neomycin resistance (ACTB-mCherry-Neo) lentivirus, both derived from human B lymphotropic viruses. Furthermore, the working concentrations necessary to achieve over 90% death in uninfected DFSCs were found to be 1 μg/mL for puromycin and 400 μg/mL for geneticin. DFSCs underwent infection using a half-volume method with these lentiviruses consecutively. Specifically, 2×10^5 DFSCs per well were seeded onto 6-well plates overnight, followed by the addition of 1 mL of medium containing the respective volume of CD63-EGFP-Puro lentivirus (according to the formula) and 10 μg of polybrene for a 4-hour infection period. Subsequently, the medium was supplemented with an additional 1 mL for continued infection. After 48 h, puromycin was added to select stable cell lines over another 48 h. DFSCs previously infected with CD63-EGFP-Puro lentivirus were then infected with ACTB-mCherry-Neo lentivirus using the same procedure and selected with geneticin for four days. This process resulted in the establishment of experimental DFSCs (E-DFSCs) lines expressing both CD63-EGFP and ACTB-mCherry proteins. Similarly, control DFSCs (C-DFSCs) were infected with Puro and Neo lentiviruses. All lentiviruses and selection agents were sourced from Hanbio Biotechnology, China.

$$V\,(lentivirus) = \frac{MOI * \ cell\ number}{Virus\ titer\,(TU/ml) * \ 1000}$$

Cell co-culture in vitro

In vitro, PDLCs and RAW264.7 cells were categorized into the following experimental groups: DFSC group, E-DFSC group, C-DFSC group, and a control group. For PDLCs migration assays, 5×10^4 PDLCs per well were seeded into the upper chambers, and either 1×10^5 DFSCs were placed in the lower wells of Transwell chambers (8 μm pore, Corning, USA). Conversely, for inducing RAW264.7 polarization, 1×10^5 DFSCs were positioned in the upper chambers (0.4 μm pore, Corning). Before the addition of DFSCs, 1×10^6 RAW264.7 cells were pretreated with 1 μg/mL lipopolysaccharide (LPS, Invitrogen) from Porphyromonas gingivalis (P. gingivalis) for 24 h. The co-culture in the Transwell system lasted for 48 h.

Cell proliferation, migration, and differentiation assay

Cell proliferation was assessed using the Cell Counting Kit-8 (CCK-8, Beyotime, China) and the Multiskan Go spectrophotometer (Thermo Fisher, USA) as described in previous studies [29]. PDLC migration was recorded and calculated following the methods outlined in prior research [29]. The relative migration rate was normalized to the control group as a standardized result.

DFSCs were cultured in the osteogenic or adipogenic medium (Syagen, China) to induce differentiation over two weeks. Staining with alizarin red and Oil Red O was carried out according to protocols established in previous studies [28–30]. The expression of relevant genes was quantified using quantitative real-time polymerase chain reaction (qRT-PCR), as detailed in earlier publications

[28–30]. Primers for the target genes are listed in Supplementary Table 1.

Flow cytometry

To evaluate surface markers, cells were incubated with fluorescein isothiocyanate (FITC)-conjugated antibodies against CD44, CD34, CD45, CD90, and CD105 from BD Biosciences (USA), or with phycoerythrin-cyanine7 (PE-Cy7)-conjugated antibodies against CD86 and allophycocyanin (APC)-conjugated antibodies against CD206 from eBioscience(USA) for 30 min at 4 °C. Fluorescence was measured using flow cytometry (Attune NxT, Thermo Fisher, USA), and data were analyzed using FlowJo software (version 10).

Animal study

Animals

Sixty-six male specific pathogen-free (SPF), eight-week-old male C57BL/6 mice were purchased from the Chengdu Dassy Experimental Animals Co., Ltd. (Tianfu Life Science Park, Chengdu, Sichuan Province, China). The animals were accommodated individually in S8 intelligent independent ventilation cages (IVC, VMU56DS8-2, Suzhou Suhang Technology Equipment Co., LTD, China) located at the State Key Laboratory of Oral Diseases, West China Hospital of Stomatology, Sichuan University. Additionally, the environment was maintained with a temperature of 22 °C and a 12 h light-and-dark cycle. The mice were reared with standard lab chow (Dassy, China) and autoclaved tap water ad libitum during the 1-week acclimatization. The conduct and findings of the papers are reported following the ARRIVE Guidelines 2.0, ensuring rigorous and transparent reporting of our animal-based research.

Periodontal defect creation and implantation

After acclimatization, C57 mice (15–25 g) were randomly divided into eight groups: healthy (n=6, no surgery), DFSC (n=6, periodontal defect+20ul 2×10^6 DFSCs), E-DFSC (n=24, periodontal defect+20ul 2×10^6 E-DFSCs), C-DFSC (n=6, periodontal defect+20ul 2×10^6 C-DFSCs), and control ((n=24, periodontal defect+20ul DPBS). Mice were anesthetized with pentobarbital (1 mg/kg, Sigma-Aldrich, USA) via intraperitoneal injection and minimized pain with buprenorphine (0.05 mg/kg, Sigma-Aldrich) for perioperative analgesia [31]. All mice, except those in the healthy group, underwent the establishment of a periodontal defect model in the right mandible. Briefly, after routine hair removal and disinfection, skin was cut and occlusal muscle was bluntly separated to expose the alveolar bone at the first to third mandibular molars' root orientation. A ball drill of 1 mm diameter was used to prepare the periodontal defect with a size of 2 mm× 1 mm× 0.5 mm (depth reaching the root surface) and the residual periodontal ligament was scraped with a curettage. Subsequently, after sterile 0.9%NaCL irrigating, 20ul cells suspension (2×10^6) or DPBS was implanted into the defect area, and muscle and skin were reduced and sutured in situ.

Postoperative management and euthanasia

As postsurgical management, 100 μg ibuprofen sustained release tablets (Taiji, Beijing, China) were performed by rectal administration for post-surgery pain control for 3 days. A soft diet(fodder mixed with autoclaved tap water) was fed for 4 weeks. Animals were euthanized with an intraperitoneal injection for pentobarbital overdose (about 500 μl). When the animals had no conscious by the toe-pinch response, their right mandibles were dissected and collected for micro-CT and histological analysis. According to the principle of 6 per group at each time point, thirty-six mice from the E-DFSC group (n=18) and control group (n=18) were sacrificed randomly on the 1st, 3rd, and 5th days for in vivo tracer detection. The residual mice were sacrificed in the 4th week.

Micro-computed tomography analysis

The right mandibles of mice were scanned using a Sky-Scan 1176 desktop X-ray micro-CT system (Bruker, Germany), following the protocol described in a previous study [32]. The images were reconstructed using NRecon and CTvox software and analyzed with DataViewers and CTan software. The region of interest (ROI) was defined to encompass 220±5 layers (8.87493 μm per layer) extending from the distal root of the first molar to the mesial root of the third molar along the X-axis, 115±5 layers from the cement-enamel junction (CEJ) to the root tip along the Y-axis, and 55±5 layers from the bone surface to the root surface along the Z-axis. Within this 3-dimensional (3D) ROI, parameters such as bone volume to total volume (BV/TV), trabecular thickness (Tb. Th), trabecular separation (Tb. Sp), and trabecular number (Tb. N) of the cancellous bone were quantified.

Histological analysis

The fixation, decalcification, and sectioning of mouse mandibles were conducted as described in a previous study [31]. Staining procedures, including Hematoxylin-Eosin (H&E, Solarbio, China), Masson's trichrome (Solarbio), Tartrate-Resistant Acid Phosphatase (TRAP, Wako, Japan), immunohistochemistry (IHC), and immunofluorescence (IF), were performed following previously established methods [29]. Quantitative analysis was conducted using ImageJ software to evaluate bone surface to total surface ratio (BS/TS) in H&E-stained sections, collagen volume fraction (CVF) in Masson-stained sections, the number of TRAP-positive osteoclasts, average optical density (AOD) in IHC, OPG/RANKL ratio in IHC, and

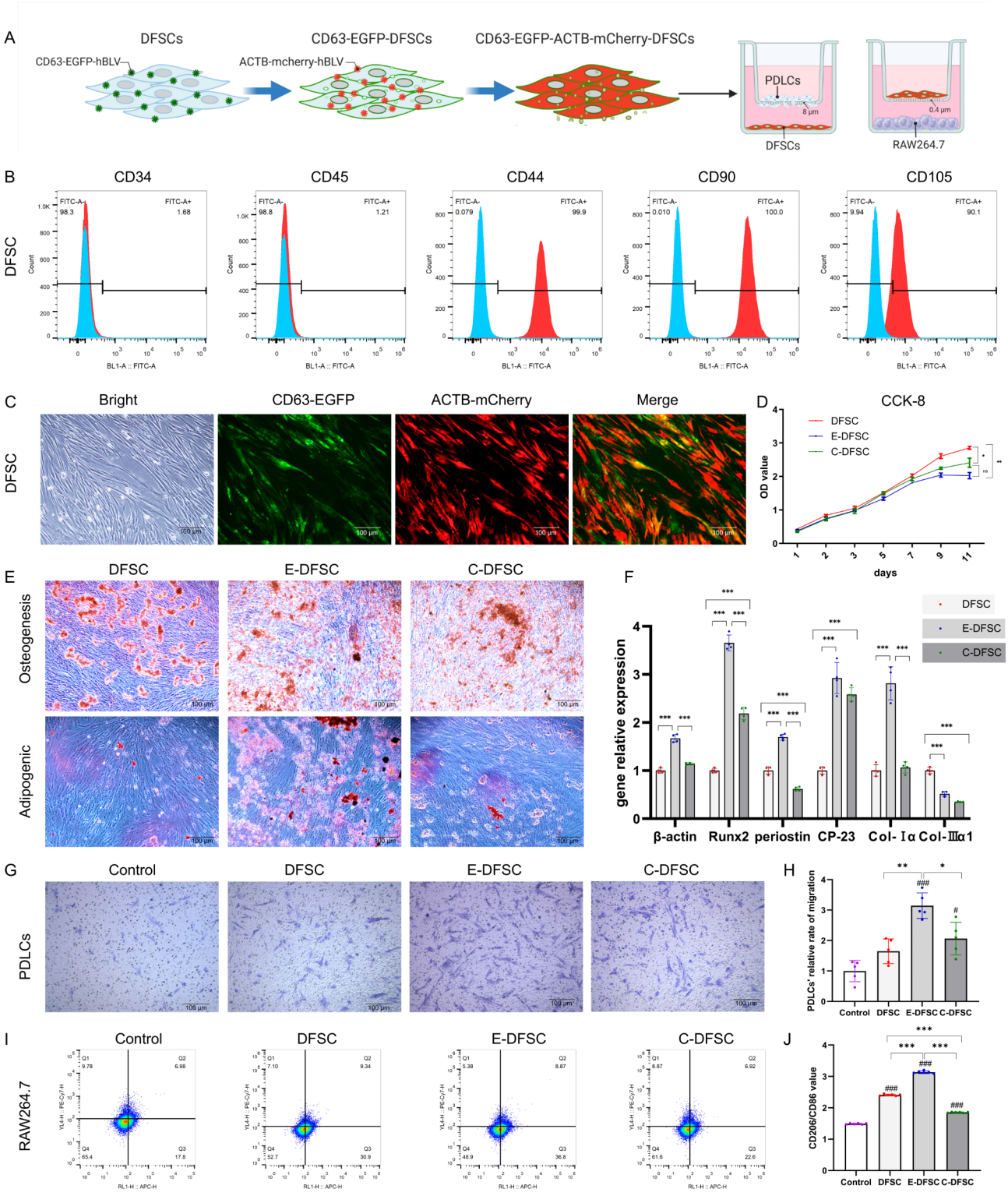

Fig. 1 (See legend on next page.)

the M2/M1 macrophage ratio in IF-stained sections as previously described [29].

Primary antibodies included anti-collagen type-Iα (Col-Iα, Abcam, USA), anti-CD68 (Abcam), anti-myeloperoxidase (MPO, R&D Systems, USA), anti-nitric oxide synthase 2 (NOS2, Santa Cruz, USA), anti-tumor necrosis factor-α (TNF-α, Santa Cruz), anti- recombinant chemokine (C-X-C-motif) receptor

(See figure on previous page.)

Fig. 1 Characteristic and functional identification of E-DFSCs. (**A**) Flow chart of experiments in vitro. (**B**) Flow cytometry detection of markers CD34, CD45, CD44, CD90 and CD105 in DFSCs. (**C**) The image of E-DFSCs in the fluorescence microscope. Scale bar: 100 μm. (**D**) The OD values of three kinds of DFSCs proliferation were tested by the CCK-8 kit at 450 nm. (**E**) The three kinds of DFSCs for alizarin red staining of osteogenesis and oil red O staining of adipogenesis after 2 weeks of induction. Scale bar:100 μm. (**F**) The qRT-PCR for osteogenesis relative gene in three kinds of DFSCs with 2 weeks induction. (**G, H**) The images and quantitative analysis of PDLCs migration without DFSCs or with three kinds of DFSCs. Scale bar: 100 μm. (**I, J**) Flow cytometric analysis for CD206 and CD86 surface markers expression on macrophages and calculation of CD206/CD86 value after co-culture without DFSCs or with three kinds of DFSCs. DFSC represents the DFSCs uninfected with any lentivirus, E-DFSC represents the DFSCs infected with lentivirus of CD63-EGFP-Puro overexpression and lentivirus of ACTB-mCherry-NEO overexpression, and C-DFSC represents the DFSCs infected with lentivirus of Puro overexpression and lentivirus of NEO overexpression. The data were analyzed by ordinary one-way ANOVA with multiple comparisons which compare the mean of each group with the mean of every other group and the Bonferroni post hoc test. "*" means statistical significance between any two groups. "#" means statistical significance between the control group with any other group. When three groups were compared in pairs, α*=α/3, * or # $p < 0.017$; ** or ## $p < 0.003$; *** or ### $p < 0.0003$. When four groups were compared in pairs, α*=α/6, * or #$p < 0.0083$; ** or ## $p < 0.0017$; *** or ### $p < 0.00017$. Error bars represent means ± SD

4 (CXCR4, Zen, USA), anti-vascular endothelial growth factor(VEGF, Abcam), anti-CD86 (Abcam), anti-CD163 (Abcam), anti-transforming growth factor-beta 2 (TGF-β2, Abcam), anti-receptor activator of NF-κB ligand (RANKL, Abcam), and anti-osteoprotegerin (OPG, Abcam). Detection of CD86 was facilitated by Alexa Fluor 488-conjugated secondary antibodies (Invitrogen, USA), while CD68, CD163, and MPO utilized Alexa Fluor 647-conjugated secondary antibodies (Invitrogen). All antibodies were diluted at a ratio of 1:200. Nuclei were stained with 4',6-diamidino-2-phenylindole (DAPI, Solarbio), and sections were visualized using confocal microscopy (Olympus, FV1000, Japan).

Statistical analysis

Statistical analyses were conducted using GraphPad Prism 9.0. Data are presented as mean ± standard error of the mean (SEM) based on at least three independent experiments. Comparisons between the two groups were performed using a nonparametric, unpaired, two-tailed Student's t-test. For pairwise comparisons between multiple groups, an ordinary one-way analysis of variance (ANOVA) was used. A *p*-value of less than α (0.05) was considered statistically significant. When handling multiple comparisons, the α was separated to control the false positives by the Bonferroni post hoc test. Compared n times, the new test level α*=α/n.

Results

Characteristic and functional identification of E-DFSCs

DFSCs expressed MSC-related markers CD90, CD105, and CD44 while lacking expression of hematopoietic cell markers CD34 and CD45 (Fig. 1B). Engineered DFSCs (E-DFSCs) infected with CD63-EGFP and ACTB-mCherry lentiviruses exhibited both red and green fluorescence under fluorescence microscopy (Fig. 1C). Furthermore, E-DFSCs demonstrated a reduction in proliferation and enhanced differentiation capacities in osteogenesis and adipogenesis compared to DFSCs (Fig. 1D, E). Notably, E-DFSCs showed significantly increased transcription of periostin and osteogenic genes, including RUNX2, CP-23, and Col-Iα (Fig. 1F). Co-culture experiments revealed that E-DFSCs significantly enhanced PDLCs migration and M2 polarization of Raw264.7 more than C-DFSCs (control lentivirus-infected DFSCs) and DFSCs, with C-DFSCs exhibiting the least effect on M2 polarization (Fig. 1G ~ H). These vitro results indicated that E-DFSCs retain similar properties to their non-engineered counterparts, but exhibit a weakened ability to proliferation and enhanced capabilities in differentiation, promotion of PDLCs migration and, macrophage immunomodulation.

E-DFSCs promote periodontal regeneration

Following the implantation of DFSCs in mice, micro-CT results at four weeks demonstrated enhanced bone regeneration in all DFSC groups compared with the control group across various indicators except the trabecular thickness (Tb. Th) (Fig. 2B ~ F). No significant differences were observed in all indicators between the cell groups *(*Fig. 2E, F*))*. The bone surface to tissue surface (BS/TS) ratios from hematoxylin and eosin (HE) staining were consistent with the bone volume fraction (BV/TV) results obtained from micro-CT (Fig. 2G, H). Compared to the control group, the mean of collagen volume fraction (CVF) from Masson's trichrome staining increased in both the DFSC and E-DFSC groups, but there were no significant differences (Fig. 2I, J). Immunohistochemical analyses revealed that the expression of Col-Iα was significantly elevated in all groups compared to the control group, and the E-DFSC group was highest (Fig. 2K, L). These results indicated that E-DFSCs have equivalent efficiency to DFSCs in periodontal defect repair and regeneration.

The implanted E-DFSCs initiate periodontal regeneration by activating endogenous cells

Immunofluorescence (IF) imaging revealed that E-DFSCs exhibited both green and dark red fluorescence (yellow box annotation in Fig. 3). Concurrently, green and light red fluorescence was observed around the nuclei of surrounding endogenous cells, potentially due to the uptake of EVs or cell debris derived from E-DFSCs (indicated by the white arrow in Fig. 3). Over time, the

number of tri-color fluorescent E-DFSCs with intact structures decreased, while the presence of fragmented E-DFSCs lacking DAPI-stained nuclei and green and light red fluorescent particles ingested by endogenous cells increased (Fig. 3D, E). These results suggested that implanted E-DFSCs might primarily activate endogenous cells through direct contact or paracrine of released EVs and other bioactive substances, thereby initiating periodontal repair in vivo. Furthermore, based on the previous research, macrophage was detected, but IF results of CD68 coupled with AF647 co-localization showed that only a few macrophages were observed on the 1st, 3rd, and 5th days (early stage) in the defect area (purple box annotation in Fig. 3). This suggested that the macrophages may not the mainly endogenous immune cells which communicated with implanted E-DFSCs at an early stage.

The implanted E-DFSCs enhance neutrophil infiltration in the early stages of injury repair

At the 1st, 3rd, and 5th days, post-implantation of E-DFSCs, hematoxylin and eosin (HE) staining (Fig. 4A ~ C) revealed abundant inflammatory cell infiltration in the defect area. Most of these cells exhibited neutrophilic characteristics, with cytoplasm that was either colorless or exhibited an extremely light red, containing dispersed light red or light purple granules. This observation was further supported by myeloperoxidase (MPO) coupled with AF647 co-localization, confirming that the majority of the cells clustered around the E-DFSCs were neutrophils (yellow box annotation in Fig. 4). Meanwhile, neutrophils also participated in EVs and debris phagocytosis from E-DFSCs (indicated by the white arrow in Fig. 4). Additionally, in periodontal defects, compared to the control group, MPO positive neutrophils in the E-DFSC group decreased on the 1st day (Fig. 4D), but significantly increased on the 3rd and 5th days (Fig. 4E, F). Moreover, MPO + neutrophils increased gradually over time in both groups (Fig. 4G, H). Preliminary in vivo tracer results indicated that neutrophils were the primary endogenous cells involved in the information exchange with implanted E-DFSCs, and E-DFSCs could enhance neutrophil infiltration during the early injury stage.

The implanted E-DFSCs induce the N2 phenotype of neutrophils in the early stages of injury repair

In order to further explore the influence of E-DFSCs on neutrophils, we measured the phenotype of neutrophils by immunohistochemistry (IHC) at the 1st, 3rd, and 5th days post-implantation of E-DFSC. As IHC results shown, compared with the control group, the expressions of proteins related to N1 phenotype, including nitric oxide synthase 2 (NOS2) and tumor necrosis factor-α (TNF-α), were significantly reduced in E-DFSC group (Fig. 5A–D), while the corresponding proteins related to N2 phenotype, chemokine (C-X-C-motif) receptor 4 (CXCR4) and vascular endothelial growth factor (VEGF), were significantly increased in E-DFSC group (Fig. 5E–H). Additionally, in E-DFSC groups, there is a tendency for the down-regulation of NOS2 and TNF-α and up-regulation of CXCR4 and VEGF over time, indicating that the implantation of E-DFSCs contributes to the sequential transformation of the N1 and N2 phenotypes of neutrophils to match the healing process of tissues. In conclusion, E-DFSCs can not only promote the local infiltration of neutrophils but also promote the phenotypic transformation of N2-type neutrophils, thereby accelerating the healing process of periodontal injury.

The implanted E-DFSCs regulate the polarization of M2-type macrophages and bone immunity in the late stage of repair

For verifying the effect on macrophages and bone immunity in the late stage of regeneration following the neutrophils' immune reaction to E-DFSCs in the early stage, the phenotype of macrophages, RANKL/OPG signaling pathway, and osteoclasts activation were examined at the 4th week after E-DFSCs implantation. Compared to the control group, the expression of TNF-α (Fig. 6A, B) was notably decreased in the E-DFSC group, while the CD163/CD86 ratio value (Fig. 6A, D) and expression of transforming growth factor-beta2 (TGF-β2) (Fig. 6A, C) observably went up, indicating the up-regulation of M2 type macrophages in E-DFSC group. The TRAP staining results mirrored the number of TRAP-positive cells in the E-DFSC group were significantly reduced compared with the control group (Fig. 6E, F); in synchronization, the expression of receptor activator of NF-κB ligand (RANKL) in E-DFSC group was less than that of the control group (Fig. 6E, G), but it was more in the expression of osteoprotegerin (OPG) and ratio value of OPG/RANKL (Fig. 6E, H, I); these implied that the OPG/RANKL signaling pathway was up-regulated and the activation of osteoclasts was inhibited in E-DFSC group. The above results showed that immune balance tilts towards healing and bone formation more in the E-DFSC group at the late stage of defect regeneration.

Discussion

The potential for clinical application of MSCs in treating periodontal disease is well-established. Several clinical studies have demonstrated that autologous MSCs can enhance relevant clinical indicators in patients with periodontal disease [33, 34]. However, the optimal selection and appropriate timing for no-autologous MSCs application remain unresolved issues. Effective and precise use of MSCs requires a thorough understanding of their

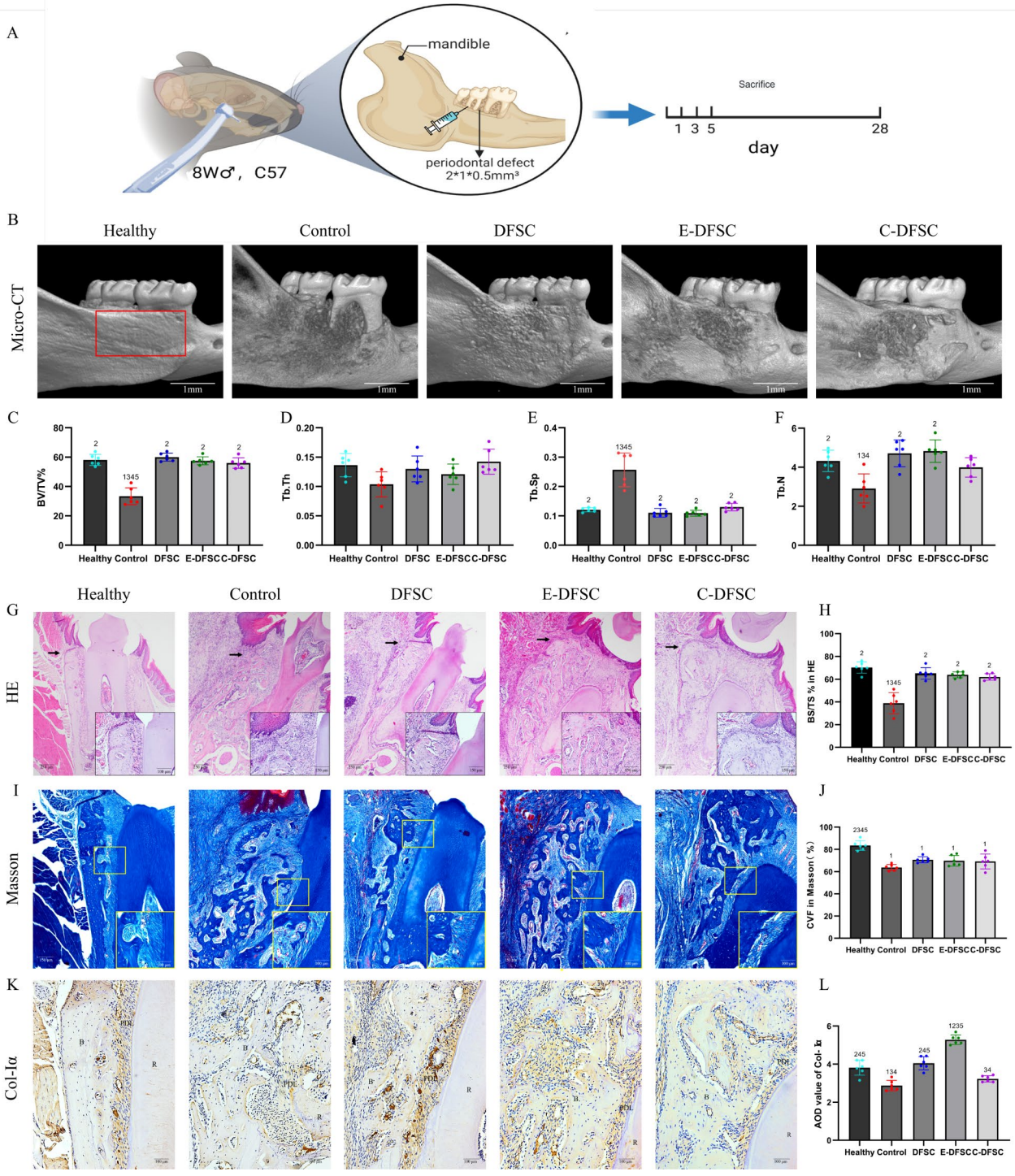

Fig. 2 E-DFSCs promote periodontal regeneration in mice at the 4th week. (**A**) Flow chart of animal experiments in vivo. (**B**) Micro-CT 3D reconstruction images of mice right mandible at 4 weeks post-treated. Scale bar: 1 mm. The red box represents the area of periodontal defect (2 mm×1 mm). **(C–F)** The values of BV/TV, Tb. Th, Tb. Sp and Tb. N from micro-CT 3D ROI. (**G, H**) The H&E staining pictures and BS/TS quantitative analysis. Scale bar: 250 μm. The black arrow points to the alveolar bone crest, in which the image was enlarged to the bottom right corner with a 150 μm scale. (**I, J**) The Masson staining pictures and CVF quantitative analysis. Scale bar: 150 μm. The yellow box indicates the periodontal ligaments in which the details were enlarged to the bottom right corner with a 100 μm scale. (**K, L**) The IHC staining images of Col-Iα and its expression quantitative analysis. Scale bar: 100 μm. Abbreviations: B, alveolar bone; R, tooth root; PDL, periodontal ligament; Healthy group treated nothing; Control group treated with 20 μl DPBS; DFSC, E-DFSC, C-DFSC groups treated with 20ul 2×10^6 corresponding cells. The data were analyzed by ordinary one-way ANOVA with multiple comparisons and the Bonferroni post hoc test. "1" means statistical significance compared to the healthy group; "2" means statistical significance compared to the control group; "3" means statistical significance compared to the DFSC group; "4" means statistical significance compared to the E- DFSC group; "5" means statistical significance compared to the C-DFSC group. Adjust α*=α/10, $p < 0.005$. Error bars represent means ± SD

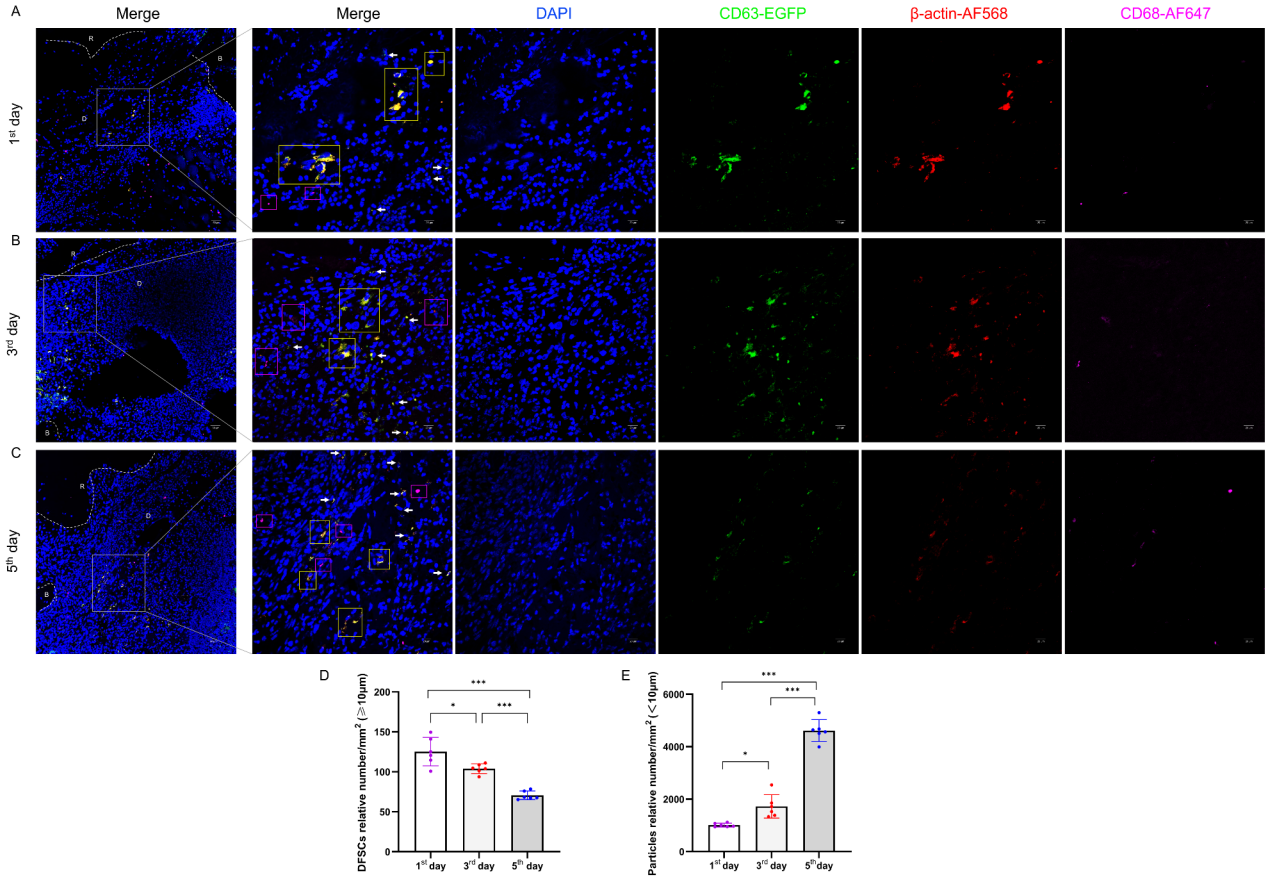

Fig. 3 The implanted E-DFSCs initiate periodontal regeneration by activating endogenous cells. (**A-C**) The images of E-DFSCs and CD68 positive macrophages on confocal after implanted into mice periodontal defect on the 1st, 3rd, and 5th days. Scale bar: 60 μm. The off-white box showed the details which were enlarged to the right images with a 20 μm scale. (**D**) Quantitative analysis of the relative number of E-DFSCs which were limited to diameter ≥ 10 μm and tri-fluorescence (red, green, and blue). (**E**) Quantitative analysis of the relative number of debris and extracellular vesicles derived from E-DFSCs which were limited to diameter <10 μm and green fluorescence. The yellow boxes circle out the DFSCs with yellow fluorescence composed of green fluorescence and red fluorescence. The white arrows point to the endogenous cells with green or chartreuse fluorescent particles. The purple boxes circle out the CD68-positive cells with purple fluorescence. Fluorescent source: blue from cell nucleus' DAPI; green from cell membranes' CD63-EGFP; red from cytoskeletons' ACTB-mCherry; purple from cell membranes' CD68-AF647. Abbreviations: B, alveolar bone; R, tooth root; D, periodontal defect. The data were analyzed by ordinary one-way ANOVA with multiple comparisons and the Bonferroni post hoc test. "*" means statistical significance between any two groups. Adjust α*=α/3, * $p < 0.017$; ** $p < 0.003$; *** $p < 0.0003$. Error bars represent means ± SD

functional mechanisms. Previous research on MSCs' mechanisms in periodontal regeneration has predominantly been results-oriented [13, 35–37]. Specific mechanisms of implanted no-autologous MSCs are still poorly understood. Given the limited survival time [9, 18] of most implanted MSCs and the potential for missing crucial information in conclusion-oriented mechanism studies, this research successfully engineered DFSC lines that enable tracking of cells in vivo, facilitating the visualization of implanted cells and their derivatives. Furthermore, the efficacy of this cell line in periodontal regeneration and immune regulation was verified both in vivo and in vitro. After implanting DFSCs into periodontal defects in mice, not only the early-stage tracks between DFSCs and innate immunity system were investigated, but also the relevant immune influences were observed at the late stage of periodontal regeneration.

In vitro studies have shown that the proliferation capacity of DFSCs decreases following lentivirus infection, consistent with earlier reports that lentiviral infection can reduce cell viability and proliferation [38, 39]. Despite this reduction in proliferation, differentiation and co-culture experiments demonstrate that the ability of infected DFSCs on multi-differentiation and promotion of PDLCs migration and M2 polarization remains robust. This discrepancy between cell proliferation and functional capabilities suggests that a decline in proliferation does not necessarily imply a reduction in other cellular functions. Furthermore, the immunomodulatory abilities of DFSCs and their capacity to mobilize indigenous cells

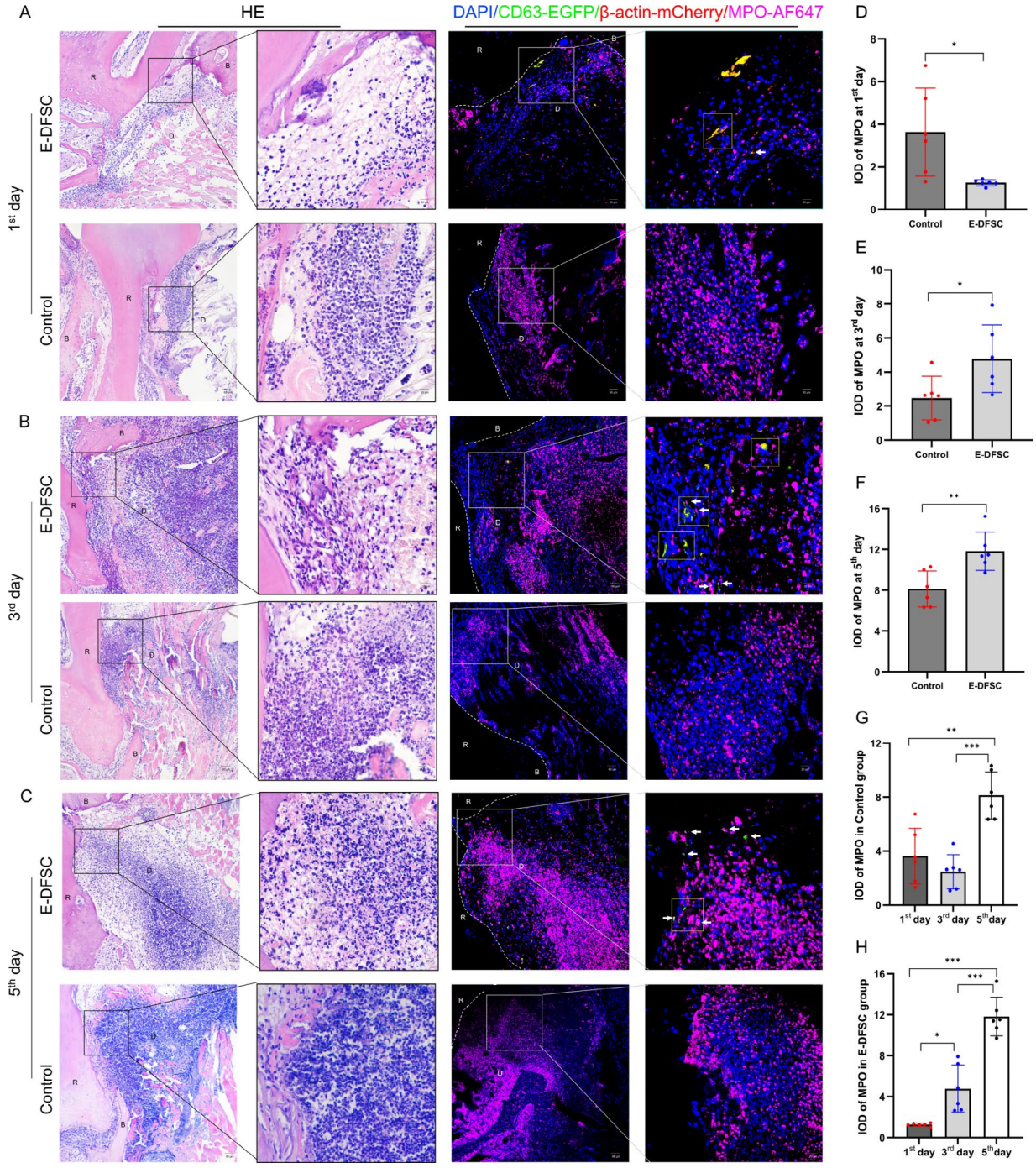

Fig. 4 The implanted E-DFSCs enhance neutrophil infiltration in the early stages of injury repair. (**A**) The pictures of H&E staining and confocal imaging on the 1st day after treatment. (**B**) The pictures of H&E staining and confocal imaging on the 3rd day after treatment. (**C**) The pictures of H&E staining and confocal imaging on the 5th day after treatment. Scale bar: 60 μm. (**D, E, F**) The MPO expression quantitative analysis on the 1st, 3rd, and 5th days in each group. (**G, H**) The MPO expression quantitative analysis in the E-DFSC group and control group over time. The black box in H&E staining pictures and the off-white box in confocal images showed the details which were enlarged to the right pictures with a 20 μm scale. The yellow boxes circle out the MPO + neutrophils clustered around the E-DFSCs. The white arrows point to the neutrophils with green or chartreuse fluorescent particles. Fluorescent source: blue from cell nucleus' DAPI; green from cell membranes' CD63-EGFP; red from cytoskeletons' ACTB-mCherry; purple from MPO-AF647. Abbreviations: B, alveolar bone; R, tooth root; D, periodontal defect; PDL, periodontal ligament. The two-tailed student's T-test was used for intergroup analysis at the same time point. "*" means statistical significance between any two groups. * $p < 0.05$; ** $p < 0.01$; *** $p < 0.001$. The ordinary one-way ANOVA and Bonferroni post hoc test were used for pairwise comparative analysis at different time points in the group. Adjust α*=α/3, * $p < 0.017$; ** $p < 0.003$; *** $p < 0.0003$. Error bars represent means ± SD

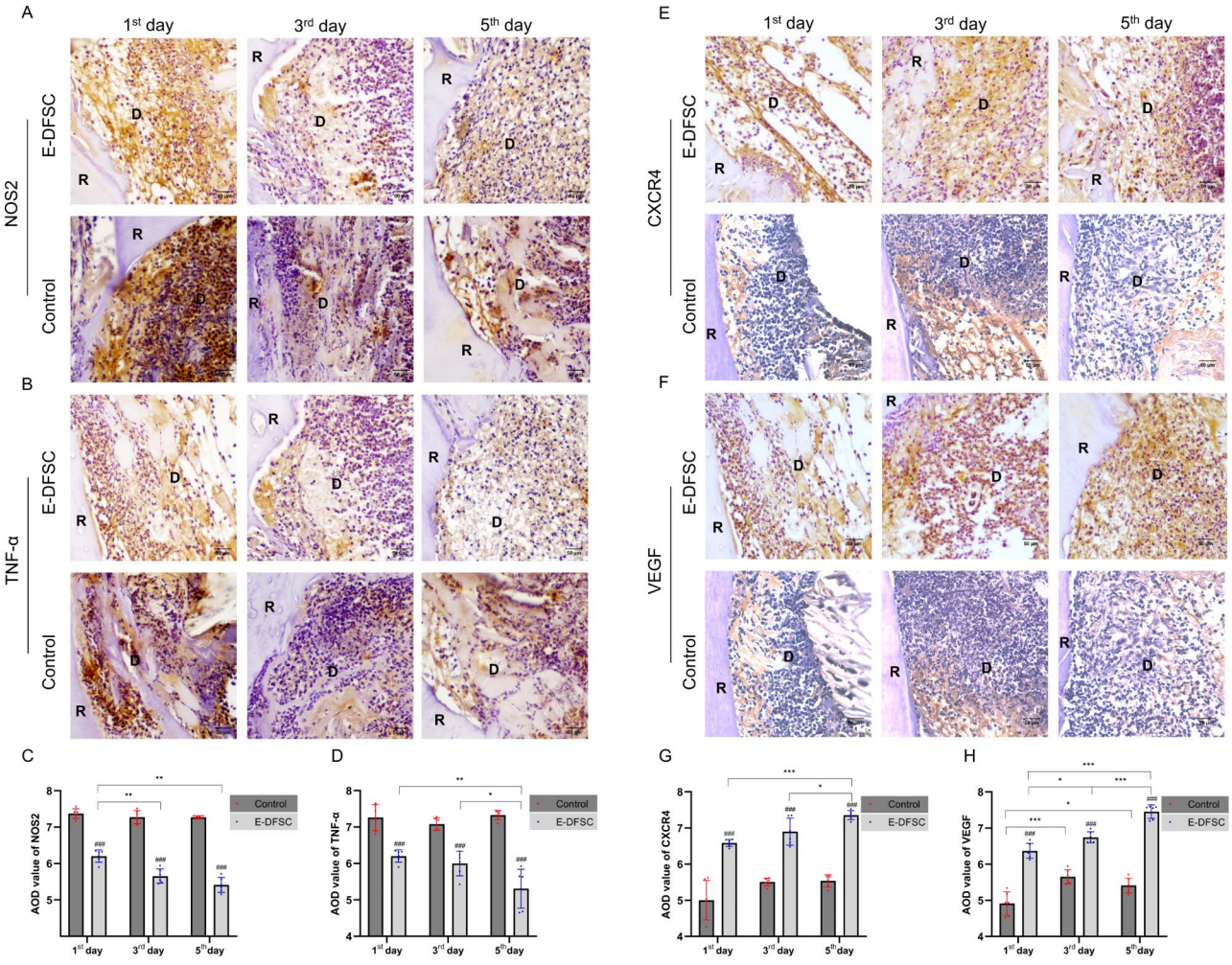

Fig. 5 The implanted E-DFSCs induce the N2 phenotype of neutrophils in the early stages of injury repair. (**A, E**) The IHC staining images of NOS2 and its expression quantitative analysis. Scale bar: 50 μm. (**B, F**) The IHC staining images of TNF-α and its expression quantitative analysis. Scale bar: 50 μm. (**C, G**) The IHC staining images of CXCR4 and its expression quantitative analysis. Scale bar: 50 μm. (**D, H**) The IHC staining images of VEGF and its expression quantitative analysis. Scale bar: 50 μm. The abbreviations, groupings, and data analysis were the same as the figuer4 legend. "#" means statistical significance between the E-DFSC group and the control group at the same time point. # $p < 0.05$; ## $p < 0.01$; ### $p < 0.001$. "*" means statistical significance among different time points in the group. Adjust α*=α/3, * $p < 0.017$; ** $p < 0.003$; *** $p < 0.0003$. Error bars represent means ± SD

may be more critical than their proliferative capacity for periodontal regeneration. This is evidenced by the observation that the repair of alveolar bone and periodontal ligaments in mice was not compromised by the diminished proliferative ability of infected DFSCs.

A detailed comparison revealed that E-DFSCs have superior performance than DFSCs in osteogenic differentiation, promoting M2 polarization and PDLCs migration, and up-regulating COL-1 expression. In previous studies, gene overexpression was used to optimize some properties of MSCs [40, 41], and the overexpression of ACTB and CD63 in DFSCs may potentially enhance the functionality of DFSCs. Beta-actin (ACTB), a highly conserved cytoskeletal structural protein, plays critical roles in cell growth and migration [42], and its ablation can modify the ratio of globular actin (G-actin) to filamentous actin (F-actin) [43], which is essential for osteogenic and adipogenic differentiation of MSCs [44]. CD63, a member of the tetraspanin superfamily, is abundantly expressed and localized to the intraluminal vesicles of late endosomes and multivesicular bodies in EVs [45]. As a common scaffold protein for target protein loading in EVs [46], CD63 enhances EVs secretion [47] and supports various biological functions, such as ferritin secretion [48] and increased biogenesis [49], thereby facilitating the exchange of information between cells. OF course, further experiments will be planned to determine whether the overexpression of ACTB and CD63 can effectively optimize the specific functionality of DFSCs.

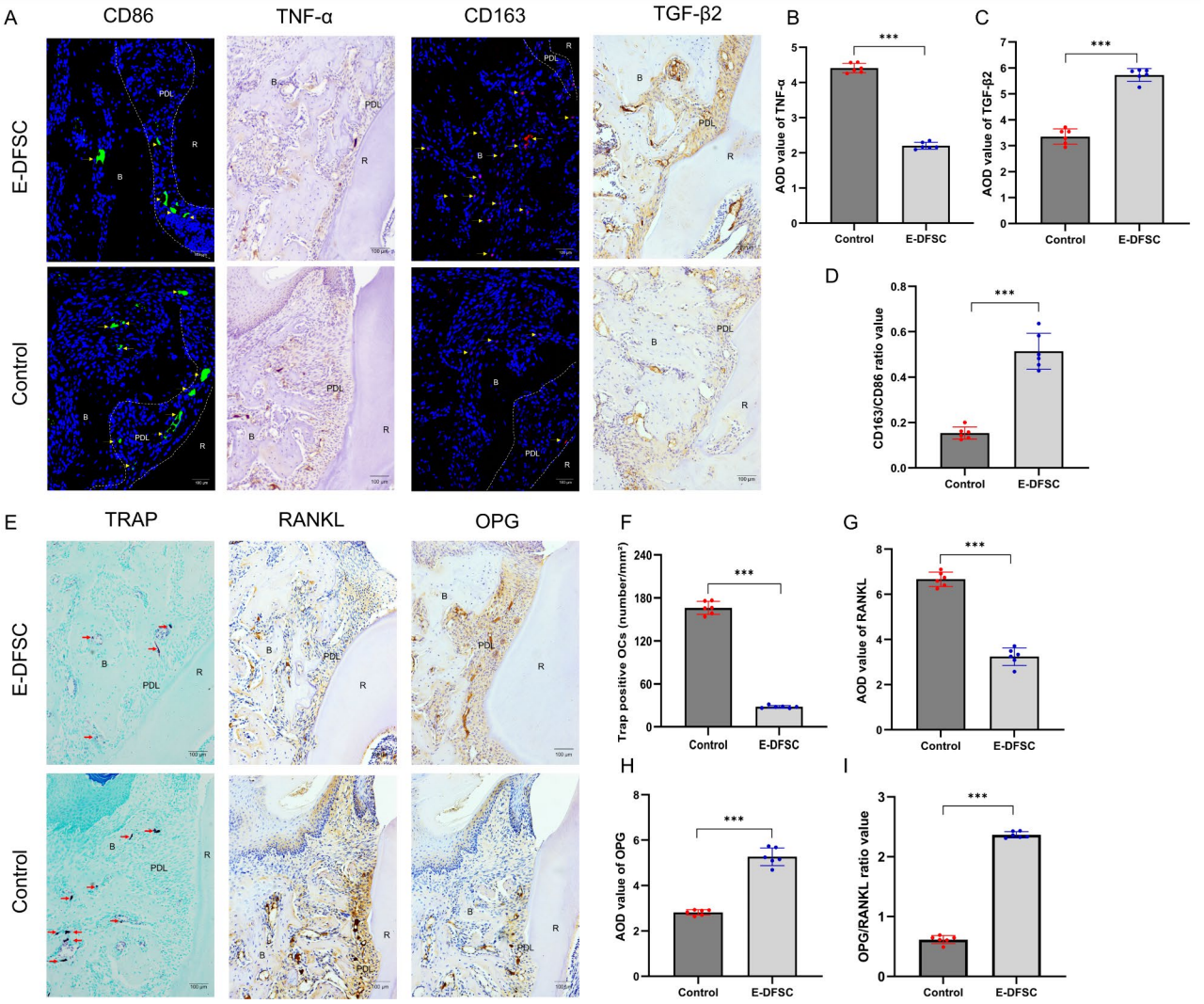

Fig. 6 The implanted E-DFSCs regulate polarization of M2-type macrophages and bone immunity in the late stage of repair. (**A**) The IF and IHC staining images of CD86, TNF-α, CD163, and TGF-β in the fourth week. Scale bar: 100 μm. Fluorescent source: blue from cell nucleus' DAPI; green from cell membranes' CD86-488; red from cell membranes' CD163-AF647. The CD86 + cells represent M1-type macrophages, and the CD163 + cells represent M2-type macrophages. (**B, C**) Quantitative analysis of TNF-α and TGF-β. (**D**) The ratio value of CD163/CD86 (M2/M1). (**E**) The TRAP staining pictures and IHC staining images of RANKL and OPG in the fourth week. Scale bar: 100 μm. The red arrows pointed to the fuchsia TRAP + osteoclasts. (**F**) The relative number of TRAP + osteoclasts. (**G, H**) Quantitative analysis of RANKL and OPG. (**I**) The ratio value of RANKL/OPG. The abbreviations, groupings, and data analysis were the same as the Fig. 4 legend. "*" means statistical significance between any two groups. * $p < 0.05$; ** $p < 0.01$; *** $p < 0.001$. Error bars represent means ± SD

Preliminary in vivo tracing results indicated no visible proliferation of DFSCs after implantation; rather, the number of structurally intact DFSCs gradually declined over time in the defect area, aligning with previous studies [9, 18]. The implanted DFSCs can interact with endogenous cells via direct contact or paracrine signaling, activating these endogenous cells to participate in tissue repair. Following the implantation of DFSCs, neutrophils, not macrophages [50] or lymphocytes [51] as previously suggested, were the primary endogenous cells that migrated to the injury site to interact with DFSCs and phagocytize sEVs. Neutrophils play a critical role in the onset, progression, and healing of periodontitis [52, 53]. As a primary line of immune defense, neutrophils exhibit robust chemotaxis, rapidly moving to inflammatory sites [54]. Upon activation, neutrophils release a range of substances, including processed antigens, chemokines, cytokines, and cytotoxic effector molecules like peroxide and superoxide, [55] which influence the subsequent immune responses of antigen-presenting cells, [56] macrophages, [19] and T lymphocytes [57]. Immune regulation is crucial for tissue regeneration. Given the limited survival time of implanted MSCs and the importance of early immune regulation for tissue healing, this study

focused on tracing the biological behavior of DFSCs in the early stage (1,3,5 days). Of course, in order to have a deeper understanding of the fate of DFSCs and their complex interactions in the whole immune system turnover process, long-term tracking of DFSCs is necessary, and we will gradually improve this huge works in subsequent experiments.

The recruitment of neutrophils is crucial for the repair of injured or inflamed tissues. Kovtun et al. [58] discovered that granulocyte colony-stimulating factor (G-CSF) significantly enhances neutrophil recruitment, thereby accelerating fracture healing; conversely, depletion of neutrophils impairs this process. Moreover, Okan et al. [59] suggested a mechanism whereby infiltrating neutrophils promote early fracture healing through the formation of an "emergency extracellular matrix (ECM)." Subsequent research has further detailed how danger-associated molecular patterns (DAMPs) released following a fracture primarily recruit neutrophils to the injury site. These chemotactic neutrophils clear the area by phagocytizing pathogens and tissue or cellular debris and facilitate the formation of a local hematoma by interacting with platelets to form neutrophil extracellular traps (NETs) [60]. Following this, neutrophils contribute to the reconstruction of the local extracellular matrix and the establishment of a vascular network, enhancing fracture healing [61]. In our study, implanted DFSCs significantly increased neutrophil recruitment in the early stages of periodontal injury, enhancing the clearance of damaged tissues or cells and the establishment of an extracellular matrix and vascular network, thereby promoting the healing of periodontal defects.

In addition to the effective infiltration of neutrophils, the transformation of the neutrophil phenotype in the injured area is also important for tissue healing. In the study on the subtype classification of neutrophils, it was demonstrated that different environmental conditions induce distinct neutrophil subtypes, such as N1 and N2 [62]. N1 neutrophils exhibit cytotoxicity, high migration, phagocytosis, oxidative bursts, and pro-inflammatory properties but lack anti-tumor and inhibitory capabilities. Conversely, N2 neutrophils are characterized by longevity, inhibitory, anti-inflammatory, and pro-tumor properties, without exhibiting cytotoxicity, migration, or phagocytic activities [63]. In research by Yonggang [64] on myocardial infarction (MI), N1 neutrophils are the predominant phenotype in the early stages of MI (comprising over 80% of total neutrophils) due to DAMPs and the inflammatory environment. Over time post-MI, the proportion of N2 neutrophils increases, underscoring their role in resolving inflammation and aiding wound repair. Similarly, in this study, we found that over time, after DFSCs implantation, the phenotypic expression of N1 neutrophils gradually decreased, while the N2 type gradually increased, indicating that the transformation of the N1 and N2 phenotypes of neutrophils matched the healing process of tissues. Importantly, the promotion of N2 phenotype transformation by DFSCs can accelerate the entire immune balance entering the anti-inflammatory and repair stage earlier and faster.

As mentioned earlier, as a primary line of immune defense, the neutrophils' phenotype transformation affects the subsequent immune response and process of tissue healing to a certain extent. Andreea's study [19] demonstrated that mediators released by neutrophil subtypes significantly influence the phenotypic modulation of macrophages. Factors released by N1 neutrophils induce macrophages to polarize towards the M1 phenotype, while exposure to the N2 secretome prompts macrophages to adopt a pro-healing M2 phenotype. In this study, after DFSCs implantation, we observed the up-regulation both of N2 neutrophils in the early stage of injury and M2 macrophages in late the stage of regeneration. However, given the few infiltrations of macrophages in the early stage, the effect of DFSCs on M2 polarization is likely to be because DFSCs promote the N2 neutrophils conversion, which makes N2 secretome increase to polarize the macrophages to M2. Of course, we need to design more accurate experiments to clarify whether there is a necessary relationship between N2 and M2 in the process of periodontal defect repair.

In addition, Wagoner [37] previously proposed the "immune clearance mechanism of dying MSCs in vivo," wherein MSCs rapidly perish post-implantation and are phagocytized by immune cells. This clearance of dying MSCs can polarize them towards an anti-inflammatory, tolerant, and regenerative phenotype, thereby modulating the immune system and facilitating tissue repair. However, this theory has been met with skepticism, as evidence suggests that the efficacy of MSCs may rely heavily on their cellular activity and adaptability [65, 66]. In our study, immune clearance occurs not only for deceased MSCs but also for xenogeneic, implanted, surviving DFSCs. The clearance of DFSCs-derived EVs and cell debris may also promote innate immune cells, such as neutrophils and macrophages, polarizing to anti-inflammatory phenotypes. The up-regulation of N2 and M2 phenotype shifted the immune balance towards tissue healing. Therefore, the ratio of OPG/RANKL was up-regulated and osteoclasts were reduced at the 4th week, thereby the bone immune balance tilts towards bone formation to promote alveolar bone regeneration.

In the immune system, the interactions and relationships among various immune cells are complex. Understanding the differential effects of MSCs on immune cells is crucial. This knowledge is essential for effectively

utilizing these cells to enhance immune balance and facilitate tissue repair and regeneration at the appropriate time.

Conclusion

In this study, we successfully developed an approach to investigate the mechanisms of exogenously implanted MSCs in vivo. The preliminary tracing results suggested that DFSCs may activate endogenous immune cells, such as neutrophils, through direct contact and indirect action. This activation primarily promotes the neutrophils' infiltration and phenotypic transformation of N2-type neutrophils in early immune responses. Meanwhile, in the late stage of regeneration, the polarization of M2-type macrophages, upregulation of OPG/RANKL signal pathway and inhibition of osteoclasts are also verified, suggesting immune balance develops in the direction of healing and bone formation. Therefore, the effects of xenogenous implanted DFSCs on neutrophils can regulate the immune balance to promote the healing and regeneration of periodontal tissue to a certain extent. This study provides a foundational understanding to elucidate the effects of xenogenous DFSCs on innate immunity, especially neutrophils, in the process of promoting periodontal regeneration, and provides a research basis for further understanding of the immune mechanisms of xenogenous DFSCs.

Abbreviations

DFSCs	Dental follicle stem cells
E-DFSCs	Engineered DFSCs infected with CD63-EGFP-Puro and ACTB-mCherry-Neo lentivirus vectors
C-DFSCs	Control DFSCs infected with Puro and Neo lentivirus vectors
EGFP	Enhanced green fluorescent protein
ACTB	β-Actin
micro-CT	Micro computed tomography
EVs	Extracellular vesicles
TRAP	Tartrate-Resistant Acid Phosphatase
OPG	Osteoprotegerin
RANKL	Receptor activator of NF-κB ligand
MSCs	Mesenchymal stem cells
BMSCs	Bone marrow stem cells
PDLCs	Periodontal ligament cells
RAW 264.7	Leukemia cellsin mouse macrophage
MOI	Multiplicity of infection
Puro	Puromycin
Neo	Neomycin
LPS	Lipopolysaccharide
CCK-8	Cell Counting Kit-8
qRT-PCR	Quantitative real-time polymerase chain reaction
RUNX2	Runt-related transcription factor 2, Col-Iα1:collagen type-Iα1, Col-IIα1:collagen type-IIα1, CP-23:cementum protein-23, GAPDH: glyceraldehyde-3-phosphate dehydrogenase
FITC	Fluorescein isothiocyanate
PE-Cy7	Phycoerythrin-cyanine7
APC	Allophycocyanin
DPBS	Dulbecco phosphate-buffered saline
ROI	Region of interest
CEJ	Cement-enamel junction
3D	Three-dimensional
BV/TV	Bone volume to total volume
Tb.Th	Trabecular thickness
Tb.Sp	Trabecular separation
Tb.N	Trabecular number
H&E/HE	Hematoxylin-Eosin
IHC	Immunohistochemistry
IF	Immunofluorescence
BS/TS	Bone surface to total surface ratio
CVF	Collagen volume fraction
AOD	Average optical density
Col-Iα	Collagen type-Iα
MPO	Myeloperoxidase
NOS2	Nitric oxide synthase 2
TNF-α	Tumor necrosis factor-α
CXCR4	Chemokine (C-X-C-motif) receptor 4
VEGF	Vascular endothelial growth factor
TGF-β2	Transforming growth factor-beta
	2:DAPI:4',6-diamidino-2-phenylindole
AF488/647	AlexaFluor488/647
G-actin	Globular actin
F-actin	Filamentous actin
G-CSF	Granulocyte colony-stimulating factor
ECM	Emergency extracellular matrix
DAMPs	Danger-associated molecular patterns
NETs	Neutrophil extracellular traps
MI	Myocardial infarction
B	Alveolar bone
R	Tooth root
PDL	Periodontal ligament
D	Periodontal defect

Supplementary Information

The online version contains supplementary material available at https://doi.org/10.1186/s13287-024-03882-2.

Supplementary Material 1

Acknowledgements

We would like to thank Fangjun Huo master for the micro-CT scan and technical guidance. We would like to express our gratitude for the support from the National Key Research and Development Program of China (2022YFA1104400) and (2021YFA1100600).

Author contributions

All authors have read and agreed to the published version of the manuscript. L.L.: conceptualization, design, and execution of the experiments, methodology, data collection and analysis, manuscript preparation, and writing. Y.W. and L.C.: sEVs isolation and identification, helped with in vivo experiments, and collected data. M.L. and J.Y.: helped with animals' experiments and collection of data. W.T.: administrative support. Y.W.: financial support, administrative support, project supervision, and expert revision. S.G.: conceptualization, design of the experiments, data analysis and interpretation, manuscript preparation, and final approval of the manuscript.

Funding

This work was supported by the National Key Research and Development Program of China (2022YFA1104400) and (2021YFA1100600). The funding bodies played no role in the design of the study and collection, analysis, and interpretation of data and in writing the manuscript.

Data availability

The data underlying this article will be shared on reasonable request to the corresponding author.

Declarations

Ethics approval and consent to participate

All human cell cultures and animal experiments conducted in this study were approved by the Ethics Committees of the West China School of Stomatology, Sichuan University (No. WCHSIRB-D-2023-422 for human dental follicle tissue acquisition and No. WCHSIRB-D-2023-038 for animal experiments). The approved project was titled "Implanted DFSCs Promote Periodontal

Regeneration by Exocrine Mechanism in Vivo."The date of approvals is November 16, 2023. Written informed consents were obtained from patients and their families who provided teeth for further research.

Consent for publication
Not applicable.

Competing interests
The authors have declared no competing interests.

Artificial intelligence
We declared that artificial intelligence is not used in this study.

Author details
[1]Engineering Research Center of Oral Translational Medicine, West China Hospital of Stomatology, Ministry of Education, Sichuan University, Chengdu, P.R. China
[2]National Engineering Laboratory for Oral Regenerative Medicine, West China Hospital of Stomatology, Sichuan University, Chengdu, P.R. China
[3]State Key Laboratory of Oral Diseases, West China Hospital of Stomatology, Sichuan University, Chengdu, P.R. China
[4]West China Hospital of Stomatology, National Clinical Research Center for Oral Diseases, Sichuan University, Chengdu, P.R. China
[5]Departments of 5 Periodontics and 6 Oral and Maxillofacial Surgery, West China Hospital of Stomatology, Sichuan University, Chengdu, P.R. China
[6]Department of Periodontics, West China Hospital of Stomatology, Sichuan University, No.14, 3rd Section, Renmin South Road, Chengdu 610041, P.R. China

Received: 12 June 2024 / Accepted: 11 August 2024
Published online: 26 August 2024

References

1. Slots J. Periodontitis: facts, fallacies and the future. Periodontol 2000. 2017;75(1):7–23.
2. Herrera D, Sanz M, Shapira L, Brotons C, Chapple I, Frese T, et al. Association between periodontal diseases and cardiovascular diseases, diabetes and respiratory diseases: Consensus report of the Joint Workshop by the European Federation of Periodontology (EFP) and the European arm of the World Organization of Family doctors (WONCA Europe). J Clin Periodontol. 2023;50(6):819–41.
3. Borsa L, Dubois M, Sacco G, Lupi L. Analysis the Link between Periodontal Diseases and Alzheimer's Disease: A Systematic Review. Int J Environ Res Public Health. 2021;18(17).
4. Graziani F, Karapetsa D, Alonso B, Herrera D. Nonsurgical and surgical treatment of periodontitis: how many options for one disease? Periodontol 2000. 2017;75(1):152–88.
5. Liu Y, Guo L, Li X, Liu S, Du J, Xu J, et al. Challenges and tissue Engineering Strategies of Periodontal-guided tissue regeneration. Tissue Eng Part C Methods. 2022;28(8):405–19.
6. Nuñez J, Vignoletti F, Caffesse RG, Sanz M. Cellular therapy in periodontal regeneration. Periodontol 2000. 2019;79(1):107–16.
7. Zhang J, Ding H, Liu X, Sheng Y, Liu X, Jiang C. Dental follicle stem cells: tissue Engineering and Immunomodulation. Stem Cells Dev. 2019;28(15):986–94.
8. Nagata M, English JD, Ono N, Ono W. Diverse stem cells for periodontal tissue formation and regeneration. Genesis. 2022;60(8–9):e23495.
9. Wei X, Guo S, Liu Q, Liu L, Huo F, Wu Y et al. Dental follicle stem cells promote Periodontal regeneration through periostin-mediated macrophage infiltration and reprogramming in an inflammatory microenvironment. Int J Mol Sci. 2023;24(7).
10. Guo S, Kang J, Ji B, Guo W, Ding Y, Wu Y, et al. Periodontal-derived mesenchymal cell sheets promote Periodontal Regeneration in Inflammatory Microenvironment. Tissue Eng Part A. 2017;23(13–14):585–96.
11. Guo S, Guo W, Ding Y, Gong J, Zou Q, Xie D, et al. Comparative study of human dental follicle cell sheets and periodontal ligament cell sheets for periodontal tissue regeneration. Cell Transpl. 2013;22(6):1061–73.
12. Bharuka T, Reche A. Advancements in Periodontal Regeneration: a Comprehensive Review of Stem Cell Therapy. Cureus. 2024;16(2):e54115.
13. Chen L, Zhu S, Guo S, Tian W. Mechanisms and clinical application potential of mesenchymal stem cells-derived extracellular vesicles in periodontal regeneration. Stem Cell Res Ther. 2023;14(1):26.
14. Singhatanadgit W, Kitpakornsanti S, Toso M, Pavasant P. IFNγ-primed periodontal ligament cells regulate T-cell responses via IFNγ-inducible mediators and ICAM-1-mediated direct cell contact. R Soc Open Sci. 2022;9(7):220056.
15. Pajarinen J, Lin T, Gibon E, Kohno Y, Maruyama M, Nathan K, et al. Mesenchymal stem cell-macrophage crosstalk and bone healing. Biomaterials. 2019;196:80–9.
16. Liu J, Chen B, Bao J, Zhang Y, Lei L, Yan F. Macrophage polarization in periodontal ligament stem cells enhanced periodontal regeneration. Stem Cell Res Ther. 2019;10(1):320.
17. Garna DF, Hughes FJ, Ghuman MS. Regulation of gingival fibroblast phenotype by periodontal ligament cells in vitro. J Periodontal Res. 2022;57(2):402–11.
18. Lu L, Liu Y, Zhang X, Lin J. The therapeutic role of bone marrow stem cell local injection in rat experimental periodontitis. J Oral Rehabil. 2020;47(Suppl 1):73–82.
19. Mihaila AC, Ciortan L, Tucureanu MM, Simionescu M, Butoi E. Anti-inflammatory neutrophils Reprogram macrophages toward a Pro-healing phenotype with increased efferocytosis capacity. Cells. 2024;13(3).
20. Torres-Ruiz J, Alcalá-Carmona B, Alejandre-Aguilar R, Gómez-Martín D. Inflammatory myopathies and beyond: the dual role of neutrophils in muscle damage and regeneration. Front Immunol. 2023;14:1113214.
21. Lu F, Verleg S, Groven RVM, Poeze M, van Griensven M, Blokhuis TJ. Is there a role for N1-N2 neutrophil phenotypes in bone regeneration? A systematic review. Bone. 2024;181:117021.
22. Phillipson M, Kubes P. The Healing Power of neutrophils. Trends Immunol. 2019;40(7):635–47.
23. Cai B, Lin D, Li Y, Wang L, Xie J, Dai T, et al. N2-Polarized Neutrophils Guide Bone mesenchymal stem cell recruitment and initiate bone regeneration: a missing piece of the bone regeneration puzzle. Adv Sci (Weinh). 2021;8(19):e2100584.
24. Yu Y, Jin H, Li L, Zhang X, Zheng C, Gao X, et al. An injectable, activated neutrophil-derived exosome mimetics/extracellular matrix hybrid hydrogel with antibacterial activity and wound healing promotion effect for diabetic wound therapy. J Nanobiotechnol. 2023;21(1):308.
25. Cianci E, Recchiuti A, Trubiani O, Diomede F, Marchisio M, Miscia S, et al. Human Periodontal stem cells release Specialized Proresolving mediators and carry Immunomodulatory and Prohealing Properties regulated by Lipoxins. Stem Cells Transl Med. 2016;5(1):20–32.
26. Misawa MYO, Silvério Ruiz KG, Nociti FH Jr., Albiero ML, Saito MT, Nóbrega Stipp R, et al. Periodontal ligament-derived mesenchymal stem cells modulate neutrophil responses via paracrine mechanisms. J Periodontol. 2019;90(7):747–55.
27. Xu X, Chen Z, Xiao L, Xu Y, Xiao N, Jin W, et al. Nanosilicate-functionalized nanofibrous membrane facilitated periodontal regeneration potential by harnessing periodontal ligament cell-mediated osteogenesis and immunomodulation. J Nanobiotechnol. 2023;21(1):223.
28. Shi W, Guo S, Liu L, Liu Q, Huo F, Ding Y, et al. Small extracellular vesicles from Lipopolysaccharide-Preconditioned Dental follicle cells promote Periodontal Regeneration in an inflammatory microenvironment. ACS Biomater Sci Eng. 2020;6(10):5797–810.
29. Liu L, Guo S, Shi W, Liu Q, Huo F, Wu Y, et al. Bone marrow mesenchymal stem cell-derived small extracellular vesicles promote Periodontal Regeneration. Tissue Eng Part A. 2021;27(13–14):962–76.
30. Huang Y, Liu Q, Liu L, Huo F, Guo S, Tian W. Lipopolysaccharide-preconditioned Dental follicle stem cells derived small extracellular vesicles treating Periodontitis via reactive oxygen Species/Mitogen-Activated protein kinase signaling-mediated antioxidant effect. Int J Nanomed. 2022;17:799–819.
31. Qian L, Shujuan G, Ping H, Li L, Weiwei S, Yafei W, et al. Wnt5a up-regulates Periostin through CaMKII pathway to influence periodontal tissue destruction in early periodontitis. J Mol Histol. 2021;52(3):555–66.
32. Liu Q, Guo S, Huang Y, Wei X, Liu L, Huo F, et al. Inhibition of TRPA1 ameliorates Periodontitis by reducing Periodontal Ligament Cell oxidative stress and apoptosis via PERK/eIF2α/ATF-4/CHOP Signal Pathway. Oxid Med Cell Longev. 2022;2022:4107915.
33. Sanchez N, Fierravanti L, Nunez J, Vignoletti F, Gonzalez-Zamora M, Santamaria S, et al. Periodontal regeneration using a xenogeneic bone substitute seeded with autologous periodontal ligament-derived mesenchymal stem cells: a 12-month quasi-randomized controlled pilot clinical trial. J Clin Periodontol. 2020;47(11):1391–402.

34. Tobita M, Masubuchi Y, Ogata Y, Mitani A, Kikuchi T, Toriumi T, et al. Study protocol for periodontal tissue regeneration with a mixture of autologous adipose-derived stem cells and platelet rich plasma: a multicenter, randomized, open-label clinical trial. Regen Ther. 2022;21:436–41.
35. Rezaei M, Jamshidi S, Saffarpour A, Ashouri M, Rahbarghazi R, Rokn AR, et al. Transplantation of bone marrow-derived mesenchymal stem cells, platelet-rich plasma, and Fibrin glue for Periodontal Regeneration. Int J Periodontics Restor Dent. 2019;39(1):e32–45.
36. Song N, Scholtemeijer M, Shah K. Mesenchymal stem cell immunomodulation: mechanisms and therapeutic potential. Trends Pharmacol Sci. 2020;41(9):653–64.
37. Wagoner ZW, Zhao W. Therapeutic implications of transplanted-cell death. Nat Biomed Eng. 2021;5(5):379–84.
38. Godlewski J, Nowicki MO, Bronisz A, Williams S, Otsuki A, Nuovo G, et al. Targeting of the Bmi-1 oncogene/stem cell renewal factor by microRNA-128 inhibits glioma proliferation and self-renewal. Cancer Res. 2008;68(22):9125–30.
39. Tsumanuma Y, Iwata T, Kinoshita A, Washio K, Yoshida T, Yamada A, et al. Allogeneic transplantation of Periodontal ligament-derived multipotent mesenchymal stromal cell sheets in canine critical-size Supra-Alveolar Periodontal defect model. Biores Open Access. 2016;5(1):22–36.
40. Kaufman S, Chang P, Pendleton E, Chandar N. MicroRNA26a overexpression hastens osteoblast differentiation capacity in Dental Stem cells. Cell Reprogram. 2023;25(3):109–20.
41. Li G, Han N, Yang H, Zhang X, Cao Y, Cao Y, et al. SFRP2 promotes stem cells from apical papilla-mediated periodontal tissue regeneration in miniature pig. J Oral Rehabil. 2020;47(Suppl 1):12–8.
42. Dugina VB, Shagieva GS, Kopnin PB. Cytoplasmic Beta and Gamma actin isoforms reorganization and regulation in Tumor cells in culture and tissue. Front Pharmacol. 2022;13:895703.
43. Bunnell TM, Burbach BJ, Shimizu Y, Ervasti JM. β-Actin specifically controls cell growth, migration, and the G-actin pool. Mol Biol Cell. 2011;22(21):4047–58.
44. Khan AU, Qu R, Fan T, Ouyang J, Dai J. A glance on the role of actin in osteogenic and adipogenic differentiation of mesenchymal stem cells. Stem Cell Res Ther. 2020;11(1):283.
45. Gandham S, Su X, Wood J, Nocera AL, Alli SC, Milane L, et al. Technologies and standardization in Research on Extracellular vesicles. Trends Biotechnol. 2020;38(10):1066–98.
46. Silva AM, Lázaro-Ibáñez E, Gunnarsson A, Dhande A, Daaboul G, Peacock B, et al. Quantification of protein cargo loading into engineered extracellular vesicles at single-vesicle and single-molecule resolution. J Extracell Vesicles. 2021;10(10):e12130.
47. Hurwitz SN, Conlon MM, Rider MA, Brownstein NC, Meckes DG Jr. Nanoparticle analysis sheds budding insights into genetic drivers of extracellular vesicle biogenesis. J Extracell Vesicles. 2016;5:31295.
48. Yanatori I, Richardson DR, Dhekne HS, Toyokuni S, Kishi F. CD63 is regulated by iron via the IRE-IRP system and is important for ferritin secretion by extracellular vesicles. Blood. 2021;138(16):1490–503.
49. Dogrammatzis C, Deschamps T, Kalamvoki M. Biogenesis of Extracellular vesicles during herpes simplex virus 1 infection: role of the CD63 Tetraspanin. J Virol. 2019;93(2).
50. Liu J, Wang H, Zhang L, Li X, Ding X, Ding G, et al. Periodontal ligament stem cells promote polarization of M2 macrophages. J Leukoc Biol. 2022;111(6):1185–97.
51. Zhang Y, Chen J, Fu H, Kuang S, He F, Zhang M, et al. Exosomes derived from 3D-cultured MSCs improve therapeutic effects in periodontitis and experimental colitis and restore the Th17 cell/Treg balance in inflamed periodontium. Int J Oral Sci. 2021;13(1):43.
52. Bassani B, Cucchiara M, Butera A, Kayali O, Chiesa A, Palano MT et al. Neutrophils' Contribution to Periodontitis and Periodontitis-Associated Cardiovascular Diseases. Int J Mol Sci. 2023;24(20).
53. Liu S, Chen Y, Jiang Y, Du J, Guo L, Xu J et al. The bidirectional effect of neutrophils on periodontitis model in mice: a systematic review. Oral Dis. 2023.
54. Kolaczkowska E, Kubes P. Neutrophil recruitment and function in health and inflammation. Nat Rev Immunol. 2013;13(3):159–75.
55. Cortés-Vieyra R, Rosales C, Uribe-Querol E. Neutrophil functions in Periodontal Homeostasis. J Immunol Res. 2016;2016:1396106.
56. Vázquez-Flores L, Castañeda-Casimiro J, Vallejo-Castillo L, Álvarez-Jiménez VD, Peregrino ES, García-Martínez M, et al. Extracellular vesicles from Mycobacterium tuberculosis-infected neutrophils induce maturation of monocyte-derived dendritic cells and activation of antigen-specific Th1 cells. J Leukoc Biol. 2023;113(6):588–603.
57. Jin H, Aziz M, Murao A, Kobritz M, Shih AJ, Adelson RP et al. Antigen-presenting aged neutrophils induce CD4 + T cells to exacerbate inflammation in sepsis. J Clin Invest. 2023;133(14).
58. Kovtun A, Bergdolt S, Wiegner R, Radermacher P, Huber-Lang M, Ignatius A. The crucial role of neutrophil granulocytes in bone fracture healing. Eur Cell Mater. 2016;32:152–62.
59. Bastian OW, Koenderman L, Alblas J, Leenen LP, Blokhuis TJ. Neutrophils contribute to fracture healing by synthesizing fibronectin + extracellular matrix rapidly after injury. Clin Immunol. 2016;164:78–84.
60. Nolan E, Malanchi I. Connecting the dots: neutrophils at the interface of tissue regeneration and cancer. Semin Immunol. 2021;57:101598.
61. Kovtun A, Messerer DAC, Scharffetter-Kochanek K, Huber-Lang M, Ignatius A. Neutrophils in tissue trauma of the skin, bone, and lung: two sides of the same Coin. J Immunol Res. 2018;2018:8173983.
62. Quail DF, Amulic B, Aziz M, Barnes BJ, Eruslanov E, Fridlender ZG et al. Neutrophil phenotypes and functions in cancer: a consensus statement. J Exp Med. 2022;219(6).
63. Sansores-España LD, Melgar-Rodríguez S, Vernal R, Carrillo-Ávila BA, Martínez-Aguilar VM, Díaz-Zúñiga J. Neutrophil N1 and N2 subsets and their possible association with Periodontitis: a scoping review. Int J Mol Sci. 2022;23(20).
64. Ma Y, Yabluchanskiy A, Iyer RP, Cannon PL, Flynn ER, Jung M, et al. Temporal neutrophil polarization following myocardial infarction. Cardiovasc Res. 2016;110(1):51–61.
65. de Witte SFH, Luk F, Sierra Parraga JM, Gargesha M, Merino A, Korevaar SS, et al. Immunomodulation by therapeutic mesenchymal stromal cells (MSC) is triggered through phagocytosis of MSC by Monocytic cells. Stem Cells. 2018;36(4):602–15.
66. Giri J, Galipeau J. Mesenchymal stromal cell therapeutic potency is dependent upon viability, route of delivery, and immune match. Blood Adv. 2020;4(9):1987–97.

Publisher's Note